

RESULTS OF LIA-2 OPERATION

P. Logachev, A. Akimov, P. Bak, M. Batazova, A. Batrakov, D. Bolkhovityanov, A. Eliseev, G. Fatkin, A. Korepanov, Ya. Kulenko, G. Kuznetsov, A. Pachkov, A. Panov, A. Starostenko, D. Starostenko, BINP SB RAS, Novosibirsk, Russia
A. Akhmetov, S. Hrenkov, P. Kolesnikov, E. Kovalev, O. Nikitin, D. Smirnov, RFNC-VNIITF, Snezhinsk, Russia

Abstract

Recent results of LIA-2 operation are presented. High quality of intense electron beam has been achieved in design intervals of energy and current. All key elements of accelerator based on domestic technology successfully passed through long term operational tests.

INTRODUCTION

Linear induction accelerators are widely used now for x-ray flash radiography of high optical density objects [1]. This particular application of linear induction accelerators is very exigent to high current electron beam quality. The value of electron beam emittance determines the minimum electron beam spot size on the target, and thus the space resolution of this method. The first experimental results of LIA-2 operation at BINP were presented three years ago [2]. Now this accelerator is successfully used for X-ray flash radiography in RFNC VNIITF [3]. High quality electron beam produced by LIA-2 together with proved reliability of new technical solutions [4], [5], [6] make a good base for full scale 20 MeV radiographic LIA project.

FEATURES OF LIA-2 OPERATION IN RADIOGRAPHIC REGIME

The radiographic regime of LIA-2 operation restricts unfortunately the maximum electron beam energy and current. This phenomenon connected with X-ray conversion target explosion and ballistic penetration of small tantalum drops into accelerating bit-slice HV insulator and LIA-2 diode. This leads to significant breakdown strength reduction both in accelerating tube and diode (see Fig. 2). Thus reliable LIA-2 operation with X-ray conversion target explosion can be held up to 1.6 MeV and 1.5 kA of electron beam energy and current. The maximum energy and current for reliable operation without target explosion were obtained at the level of 2 MeV and 2 kA. It corresponds to design values. X-ray conversion target is placed at 3.9 m from the cathode. Electron beam energy deposition in 0.5 mm thick tantalum target for 1.6 MeV, 1.5 kA, 200 ns can be calculated as 230 J (1 MeV of energy loss per electron). It corresponds to 5000 K of melted target part on Fig.1 and about 1 bar of saturated vapor pressure of tantalum. There is a maximum size of hole in the target for fixed beam energy, current and pulse duration (in the case of increasing of the beam diameter on the target, the hole does not appear). For this particular case the maximum diameter of the hole is equal to 6 mm (see Fig. 1 and 4).

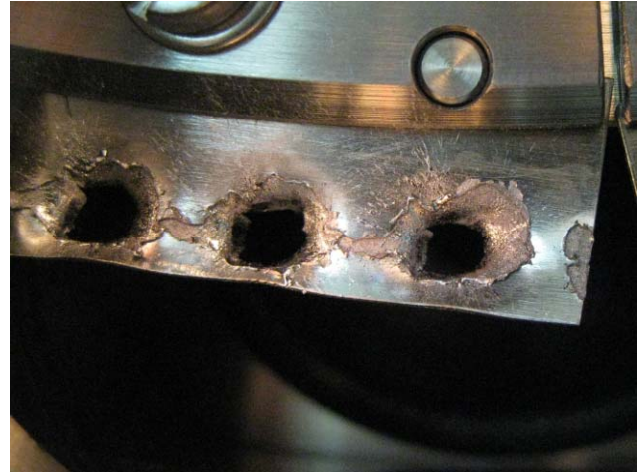


Figure 1: Maximum hole diameter in 0.5 mm thick tantalum target for 1.6 MeV, 1.5 kA, 200 ns electron beam.

In the case of the best focusing of electron beam on the target the minimum hole diameter is 1 mm (see Fig. 4) and peak tantalum temperature is about 200000 K. This is target explosion.



Figure 2: Damage of the central part of LIA-2 cathode by tantalum drops from the target. View on the cathode through the anode aperture.

The damage of the cathode central part due to target explosion (see Fig. 2) leads to emission degradation from

the cathode centre and thus to significant changes of diode optics.

This effect increases the beam spot size on the target and brings us to change the cathode after about 3000 radiographic pulses.

ELECTRON BEAM SIZE MEASUREMENT ON THE TARGET

In the case of Gaussian transverse distribution of power dissipation in the target

$$\xi = \xi_0 e^{-\frac{r^2}{2\sigma_r^2}} \quad (1)$$

(here σ_r is electron beam transverse sigma on the target, ξ – surface density of power dissipation in the target) one can get the total energy deposition Q_0 per pulse:

$$Q_0 = 2\pi\sigma_r^2 \xi_0 = \text{const} \quad (2).$$

For LIA-2 radiographic operation case (1,6 MeV, 1,5 kA, 200 ns, 0,5 mm Ta target) $Q_0=230$ J. Let us assume that power density on the border of solid metal and hole in the target made by electron beam keeps constant upon electron beam radius on the target. This assumption is based on the dominance of local conditions in the process of metal melting and evaporation. The reality is more complicated. Power deposition in the target is not uniform also in longitudinal direction. It happens due to significant initial angle of beam divergence after focus plane and due to multiple scattering in the target, so the tantalum vapor pressure on the front side of the target is higher then one on the back side. It leads to appearance of big average force in the direction of electron beam propagation. This force increases the diameter of the hole in the target in comparison with the case of uniform longitudinal beam power deposition in the target. This effect is seen clearly on the holes of the target, holes borders are turned out in the direction of electron beam propagation. So the suggested model provides an upper estimation of electron beam transverse size on the target.

$$\xi_e = \xi_0 e^{-\frac{r_e^2}{2\sigma_r^2}} = \text{const} \quad (3),$$

where ξ_e - edge value of surface power density on the target, r_e . is the target hole radius.

Simple combination of equations (2) and (3) shows that there is a maximum r_e for fixed values of Q_0 and ξ_e . This r_e corresponds to the maximum possible hole diameter for fixed value of Q_0 . Thus ξ_e can be derived from maximum $r_{e\text{max}}$ and Q_0 :

$$\xi_e = \frac{Q_0}{\pi r_{e\text{max}}^2 e} \quad (4),$$

where $e=2.718282\dots$

Combining equations (2) and (3) one can obtain:

$$\frac{\pi r_e^2 \xi_e}{Q_0} = \frac{r_e^2}{2\sigma_r^2} e^{-\frac{r_e^2}{2\sigma_r^2}} \quad (5).$$

Solving nonlinear equation (5) one can get transverse electron beam size σ_r as a function of target hole diameter ($2r_e$). Electron beam radius (FWHM/2) can be determined as $r_b = \sigma_r \sqrt{2 \ln 2}$.

Fig. 3 represents r_b as a function of target hole diameter for different values of maximum target hole diameter.

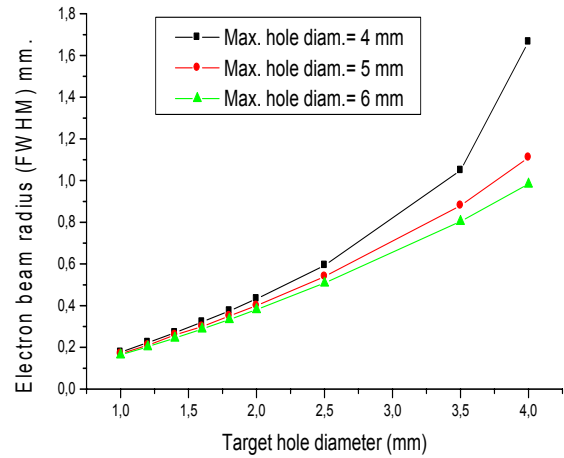


Figure 3: The dependences of electron beam radius (FWHM) upon the target hole diameter for different values of maximum target hole diameter..

In the range of target hole diameters between 1 and 1,5 mm. the solution of equation (5) is not very sensitive to the maximum target hole diameter. Fig. 4 shows minimum (1 mm) and maximum (6 mm) target hole diameters for 1.6 MeV, 1.5 kA, 200 ns LIA-2 electron beam and 0.5 mm thick tantalum target.

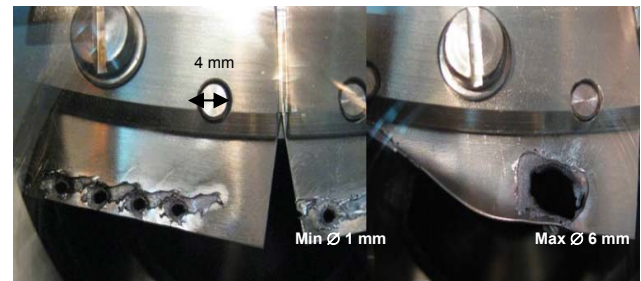


Figure 4: Minimum (1 mm) and maximum (6 mm) target hole diameters for 1.6 MeV, 1.5 kA, 200 ns LIA-2 electron beam and 0.5 mm thick tantalum target.

Finally, using Fig. 3, one can get transverse electron beam radius (FWHM) 0.17 mm for 1 mm target hole diameter.

BEAM EMMITTANCE ESTIMATION

The beam emittance estimation can be performed using the electron beam convergent angle just before the target. Electron beam structure for LIA-2 was calculated precisely by UltraSAM code developed in BINP [7]. The result is presented on Fig. 5 and 6.

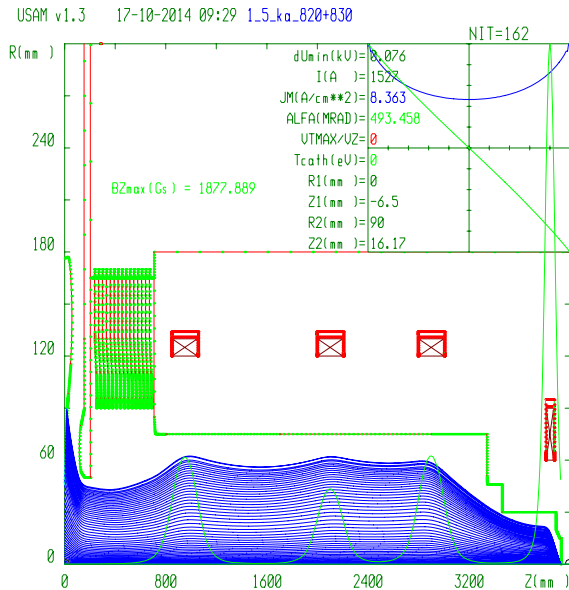


Figure 5: Electron beam envelope in LIA-2 for 1.6 MeV, 1,5 kA from the cathode to the target. UltraSAM simulation.

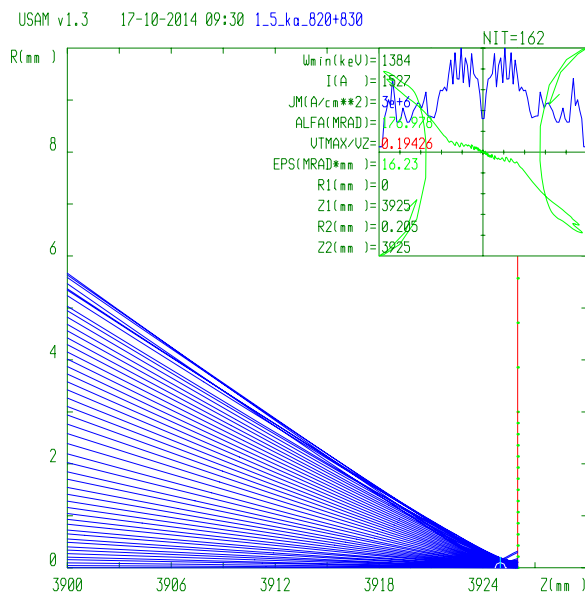


Figure 6: Electron beam envelope near the target for 1.6 MeV, 1,5 kA. UltraSAM simulation.

For this particular case the beam convergent angle on the target is 219 mrad, thus LIA-2 normalized beam emittance is less than $117 \pi \text{ mm}\cdot\text{mrad}$.

ACKNOWLEDGMENTS

This work is supported by State corporation “Rosatom” and Ministry of education and science of RF.

REFERENCES

- [1] K. Takayama, R. J. Briggs (editors) *Induction Accelerators*, Springer, 2011, ISSN 1611-1052.
- [2] P. V. Logachev et al., “Performance of 2 MEV, 2 Ka, 200 ns linear induction accelerator with ultra low beam emittance for X-ray flash radiography,” in *Proc. of 2nd Int. Particle Accelerator Conference (IPAC'2011)* (San Sebastian, Spain, 2011).
- [3] A. Akhmetov, S. Khrenkov, P. Kolesnikov, E. Kovalev, O. Nikitin, D. Smirnov, LIA-2 and BIM accelerators as part of radiographic complex at RFNC-VNIITF. RuPAC-2014, October 6-11, 2014, Obninsk, Russian Federation.
- [4] A. V. Akimov, V. E. Akimov, P. A. Bak, et al., “A pulsepower supply of the linear induction accelerator,” *Instrum. Exp. Tech.* **55** (2), 218 (2012).
- [5] P. V. Logachev, G. I. Kuznetsov, A. A. Korepanov, et al., LIA_2 linear induction accelerator, *Instrum. Exp. Tech.* **56** (6), 672 (2013).
- [6] A. V. Akimova, P. V. Logachova, A. A. Korepanova, F. V. Averin, O. V. Savinova, G. L. Mamaeva, S. L. Mamaev, Magnetic Cores Made of an Amorphous Tape for the Induction Accelerator. *Instruments and Experimental Techniques*, 2012, Vol. 55, No. 2, pp. 268–273. © Pleiades Publishing, Ltd., 2012.
- [7] A. Ivanov, M. Tiunov, ULTRASAM - 2D Code for Simulation of Electron Guns with Ultra High precision *Proc. 8th European Particle Accelerator Conference (EPAC 2002)*, Paris, France, 3-7 June 2002, p.1634-1636.